Journal of Pharmaceutical and Biomedical Analysis 180 (2020) 113035

Contents lists available at ScienceDirect

Journal of Pharmaceutical and Biomedical Analysis

journal homepage: www.elsevier.com/locate/jpba

Short communication

# Analysis of cetuximab N-Glycosylation using multiple fractionation methods and capillary electrophoresis mass spectrometry

Csaba Váradi[a,*], Craig Jakes[b,c], Jonathan Bones[b,c]

[a] Faculty of Materials Science and Engineering, Department of Chemistry, University of Miskolc, 3515 Hungary
[b] Characterisation and Comparability Laboratory, NIBRT – The National Institute for Bioprocessing Research and Training, Foster Avenue, Mount Merrion, Blackrock, Co. Dublin, A94 X099, Ireland
[c] School of Chemical and Bioprocess Engineering, University College Dublin, Belfield, Dublin 4, D04 V1W8, Ireland

ARTICLE INFO

*Article history:*
Received 26 September 2019
Received in revised form 2 December 2019
Accepted 5 December 2019
Available online 7 December 2019

*Keywords:*
Cetuximab glycosylation
Charge variants
Capillary electrophoresis
Peptide mapping

ABSTRACT

Site-specific glycosylation of Cetuximab was characterized in this study using multiple fractionation methods and capillary electrophoresis coupled to mass spectrometry (CE-MS) based glycomics. IdeS digested Cetuximab with subsequent reduction was fractionated using reversed-phase chromatography resulting in 3 fragments; Fd, Lc and Fc/2. Glycan release of the different fragments was performed in $^{18}O$ enriched water providing the possible quantification of site occupancy. 2-AA labelled glycan structures were annotated by CE-MS profiling in combination with exoglycosidase sequencing, revealing potential structures with terminal α-galactose and N-glycolyl-neuraminic acid (NGNA) mainly originating from the Fd fragment. Glycosylation analysis was also performed on different charge variants of Cetuximab that were separated using pH gradient cation-exchange chromatography to investigate the impact of glycosylation on the net charge of the protein.

© 2019 Elsevier B.V. All rights reserved.

## 1. Introduction

The main tools of targeted biological therapies are monoclonal antibodies (mAbs), which aim to block signaling pathways either *via* direct receptor binding or by binding to the ligands of receptors, thereby suppressing receptor-ligand interactions [1]. MAbs are complex molecules due to their molecular size and the high number of possible micro heterogeneities introduced through posttranslational modifications of the primary sequence, such as deamination, oxidation, C-terminal lysine variation, N-terminal pyroglutamate formation, glycation and glycosylation [2]. One of the first chimeric mouse-human antibodies targeting epidermal growth factor receptor (EGFR) was Cetuximab [3]. EGFR is a transmembrane receptor that is activated by epidermal growth factor (EGF) resulting in the auto phosphorylation of its intracellular tyrosine-kinase domain [4]. The activated tyrosine kinase is responsible to initiate signal-transduction pathways such as phosphatidil-inositol-3-phosphate and Ras signaling to induce cell proliferation [5]. Besides blocking ligand binding, Cetuximab also induces EGFR internalization and degradation resulting in the downregulation of the receptor. The EGFR receptor is often overexpressed in cancer cells resulting in continuous proliferation [6]. Blocking EGFR by Cetuximab is reported to be efficient in the inhibition of tumor progression [7]. In the European Union (EU) and United States (US), Cetuximab is used for the treatment of colorectal, head and neck cancer [8,9]. When combined with chemotherapy, Cetuximab has also extended the survival rate in non-small cell lung cancer [10,11].

Similarly to other mAbs, post-translational modifications have crucial importance in the efficacy and safety of this drug [12]. Cetuximab has reportedly two N-linked glycosylation sites at Asn 88 and Asn 299 of its heavy chain, where mainly α1-6 fucosylated structures are connected, which can be terminated in α1-3 galactose or/and N-glycolyl-neuraminic acid (NGNA) [13]. It was also found that glycans with α-Gal and NGNA are mainly originated from the Fab fragment while the Fc glycans are typically core-fucosylated bi-antennary structures with 0, 1 or 2 β-galactose residues [14]. Deglycosylated Cetuximab has no *in vitro* affinity to $Fc_{\gamma}RI$ and $Fc_{\gamma}RIIIa$ receptors and its ADCC (antibody-dependent cellular cytotoxicity) activity is lost suggesting that the N-glycans are critical quality attributes of this therapeutic protein [15].

MAbs have a large number of sub-variants that originate from post-translational modifications, such as glycosylation. Based on the monosaccharide composition of the presented glycan, the protein surface charge characteristics might differ, resulting in altered biological activity. It has been reported that the acidic, main and basic variants of Cetuximab have different affinity to $Fc_{\gamma}RIIIa$

* Corresponding author.
*E-mail address:* kemcsv@uni-miskolc.hu (C. Váradi).

https://doi.org/10.1016/j.jpba.2019.113035
0731-7085/© 2019 Elsevier B.V. All rights reserved.

receptor and altered ADCC activity [2]. Glycoforms with terminal alpha-galactose were also reported to result in hypersensitivity reactions and anaphylaxis in treated patients [16]. Thus, identification of potential glycosylation sites and annotation of the presented structures is critical, yet extremely challenging for the field of glycoanalytics [17]. A well-established strategy to identify unknown glycosylation sites and quantify site occupancy is the glycan release method by using PNGase F or A performed in heavy oxygen ($^{18}O$) enriched water. PNGase F digestion in the presence of heavy water can result in a +2.9840 Da mass shift due to the incorporation of $^{18}O$ into the aspartic acid formed during the deglycosylation reaction allowing the differentiation of glycosylation sites and deamidation occurring through some other mechanism [18].

In this study, site-specific glycosylation of Cetuximab was characterized using multiple fractionation and digestion strategies. N-glycan structures of Cetuximab were annotated by multiple exoglycosidase digestion steps in combination with CE-MS. To identify the origin of the N-glycans on Cetuximab, reverse phase chromatography was used to fractionate the resulting Fc/2, Lc and Fd fragments of Fabricator digested and reduced Cetuximab followed by glycan release in $H_2{}^{18}O$. Individual charge variants of Cetuximab were also fractioned by a pH gradient elution using strong cation exchange chromatography, showing different distribution of the glycan species across the charge variants.

## 2. Materials and methods

### 2.1. Chemicals and reagents

Isopropanol, ammonium-hydroxide, acetic acid, sodium-cyanoborohydride, 2-aminobenzoic acid, dithiothreitol (DTT), iodoacetamide (IAA) and 10 kDa molecular weight cut off (MWCO) centrifugal filters were purchased from Sigma-Aldrich (St. Louis, MO, USA). Exoglycosidase enzymes were obtained from Prozyme (San Francisco, CA, USA). Fabricator was purchased from Genovis (Lund, Sweden), $H_2{}^{18}O$ was from CK Isotopes (Leicestershire, UK).

### 2.2. C4 reverse phase chromatography

Reverse phase chromatography was performed using a Thermo Scientific Vanquish UHPLC and a Thermo Scientific MabPAc reversed phase (RP) column (4 μm, 2.1 mm × 50 mm) using 300 μg of Fabricator digested and reduced Cetuximab. The gradient used for the analysis was 95-20% Buffer A with 0.3 mL/min in 63 min (Buffer A: 0.1 % Formic acid in water, Buffer B: 0.1 % Formic acid in 60/40 Acetonitrile/Isopropanol). The detection wavelength was set to 280 nm. The sample injection volume was 15 μL where the sample temperature was 10 °C. The column temperature was 50 °C.

### 2.3. N-Glycan release in $H_2{}^{18}O$, labelling and clean-up

The collected protein fractions were denatured using 8 M urea in 0.1 M tris buffer pH 8.0 (UA solution) and subsequently reduced and alkylated using 10 mM DTT and 55 mM IAA prepared in UA solution, respectively. 100 μL of 50 mM ammonium-bicarbonate was dried by vacuum centrifugation and reconstituted in 100 μL $H_2{}^{18}O$. The denaturated protein fragments were buffer exchanged into the heavy water solution followed by N-glycan release using 500 Units of PNGase F (New England Biolabs Ipswich, MA, USA) overnight at 37 °C. The released glycans were collected from the deglycosylated proteins by centrifugation through 10 kDa MWCO filters and reduced to dryness using vacuum centrifugation (Thermo Fisher Scientific, Waltham, MA, USA). Glycans were reconstituted in 20 μL of 1% v/v aqueous formic acid to promote hydrolysis of the glycosylamines and reduced to dryness. 5 μL labelling solution (0.37 M 2-AA containing 1 M $NaCNBH_3$ in DMSO/acetic acid (70:30)) was added to the dried sugars and incubated at 65 °C for 5 h. 10 μL HPLC grade water was added to the labelled samples and then purified using frontal HILIC chromatography on a Thermo Scientific Ultimate 3000 UHPLC system (Germering, Germany) and a 50.0 × 2.1 mm ID, 1.7 μm Waters BEH Glycan amide column (Milford, MA, USA). Samples were loaded onto the column and washed to remove excess 2-AA in 85 % v/v acetonitrile. Purified glycans were eluted using 20% v/v aqueous acetonitrile, automatically collected and reduced to dryness using vacuum centrifugation prior to instrumental analysis.

**Table 1**
Mass Spectrometry Tunefile parameters.

| | |
|---|---|
| Sheath Gas | 40 |
| Aux Gas | 10 |
| Spray Voltage | 3.50 kV |
| Capillary Temperature | 320°C |
| Auxiliary Gas Heater Temperature | 400°C |

### 2.4. Trypsin digestion

100ug of Cetuximab was digested using a Kingfisher Duo Prime and magnetic SMART Digest trypsin functionalised beads from Thermo Fisher Scientific. Samples were digested for 45 min at 70 degrees. The resulting peptides were reduced with 10 mM DTT for 30 min at 57 °C and alkylated with 20 mM IAA in darkness for 30 min at room temperature. Reactions were quenched with DTT and TFA (trifluoroacetic acid) before being analysed by LC-MS.

### 2.5. Peptide mapping

Peptide mapping analysis was performed on a Thermo Scientific Q-Exactive Plus hybrid quadrupole Orbitrap mass spectrometer (Thermo Scientific, Bremen, Germany) using a Thermo Scientific Acclaim RSLC 120 C18, 2.2 μm 120 Å, 2.1 × 250 mm, using 98 to 60 % Buffer A at 0.3 mL/min over 45 min (Buffer A: 0.1% Formic acid in water, Buffer B: 0.1 % Formic acid in acetonitrile). The sample injection volume was 5 μL where the sample temperature was 5 °C. The column temperature was 25 °C. The MS was operated in positive ion mode and the data acquisition scan range was set between 200−2000 *m/z*. Full MS data was acquired at 70,000 resolution with an AGC target of 3e6. Maximum injection time was 100 ms with 1 microscan performed. Data dependent tandem mass spectrometry (dd-MS/MS) data was acquired at 17,500 resolution with an AGC target of 1e5. Maximum injection time was 200 ms with a loop count and TopN of 5. Isolation window was set to 2.0 *m/z* and NCE/stepped NCE was 28. A 7 s dynamic exclusion was applied. The MS tune parameters are outlined in Table 1.

### 2.6. Charge variant analysis

Charge fractionation was performed on a Thermo Scientific Vanquish UHPLC instrument using a Thermo Scientific MAbPac SCX-10 RS column (5 μm, 2.1 × 250 mm) with a 20–80% gradient of Buffer B in 50 min (Buffer A: CX-1 pH gradient Buffer A, pH 5.6, Buffer B: CX-1 pH gradient Buffer B, pH 10.2). Detection wavelength was 280 nm. The sample injection volume was 15 μL where the sample temperature was 10 °C. The column temperature was 50 °C.

### 2.7. CE-MS analysis

CE-MS separations were carried out on an Agilent 7100 capillary electrophoresis system with an Agilent G1607B orthogonal coaxial sheath sprayer connected to an Agilent 6520 Accurate-Mass Q-TOF mass spectrometer controlled by Mass Hunter acquisition

software, version B.07.00. (Santa Clara, CA, USA). Sample injections were obtained by pressure (100 mbar, 10 s) and electrophoretic separations were applied using −30 kV. 30 mM ammonium acetate (pH 5) was used as background electrolyte. Stable electrospray was maintained by a sheath flow of 0.2% v/v ammonium hydroxide in 50% v/v aqueous isopropanol at a flow rate of 5 μL/min by an Agilent G1376 capillary pump. The electrospray voltage was 3.2 kV while the fragmentor voltage offset was 175 V and the drying gas temperature was 250 °C delivered at 5 L/min. Mass spectra was collected using negative ionisation mode over the acquisition range of 500−2000 *m/z* with 2 GHz digitisation.

### 2.8. Data processing and analysis

Peptide mapping data was analysed by Thermo Fisher Scientific Xcalibur and further processed by Thermo Fisher Scientific BiopharmaFinder version 2.0. CE-MS glycan data was processed by Mass Hunter Qualitative Analysis B.07.00.

## 3. Results

Site-specific glycosylation of Cetuximab was characterized in this study using multiple fractionation and digestion strategies. Glycan structures of Cetuximab were annotated by multiple exoglycosidase digestion steps in combination with CE-MS profiling. Site-specificity was identified using reversed-phase fractionation of Fabricator digested and reduced Cetuximab. The glycosylation pattern was also examined across Cetuximab charge variant isoforms using cation-exchange chromatography with linear pH gradient elution followed by CE-MS profiling.

### 3.1. N-glycan structure identification

Our recently developed dynamic capillary coating based separation method was applied to characterize 2-AA labelled N-glycans from Cetuximab using CE-MS profiling and subsequent exoglycosidase sequencing [19]. Glycans were released from 200 μg of Cetuximab and sequentially digested by sialidase (*Arthrobacter ureafaciens*), α1-3/4 fucosidase (Almond Meal), α1-6 fucosidase (Bovine kidney), α-galactosidase (Coffee bean) and β-galactosidase (Jack bean) (Fig. 1). 24, mainly bi-antennary, α1-6 fucosylated structures were identified with terminal NGNA and various degrees of α- and β-galactosylation. Low quantities (>1%) of antennary fucosylated complex glycans and hybrid structures were also detected. The list of N-glycans identified on Cetuximab using the outlined approach is shown in Table 2 [13]. Due to the high advantage of CE in isomer separation, isobaric structures with identical mass (*e.g.* FA2G1GA1 and FA2G2 are both *m/z* 952.75) were also differentiated based on differences in migration time. This has crucial importance in the safety of monoclonal antibodies as terminal α-linked galactose was found to be responsible for hypersensitivity reactions and anaphylaxis in treated patients [20].

### 3.2. Site specificity and occupancy

Reversed-phase chromatography was applied to determine the origin of the identified glycans using Fabricator digested and reduced Cetuximab resulting Fc/2, Lc and Fd fragments (Fig. 2A). N-glycan release was performed in $H_2{}^{18}O$ allowing the identification of potential glycosylation sites and site occupancy. CE-MS profiling showed that NGNA and α-Gal containing structures are mainly originating from the Fab portion while the Fc glycans are mainly bi-antennary α1-6 fucosylated structures with various degrees of galactosylation (Fig. 2B). These findings are in agreement with previous studies as Qian et al. reported that Cetuximab Fc glycans are typical of IgGs while the Fab glycans have higher complexity [13].

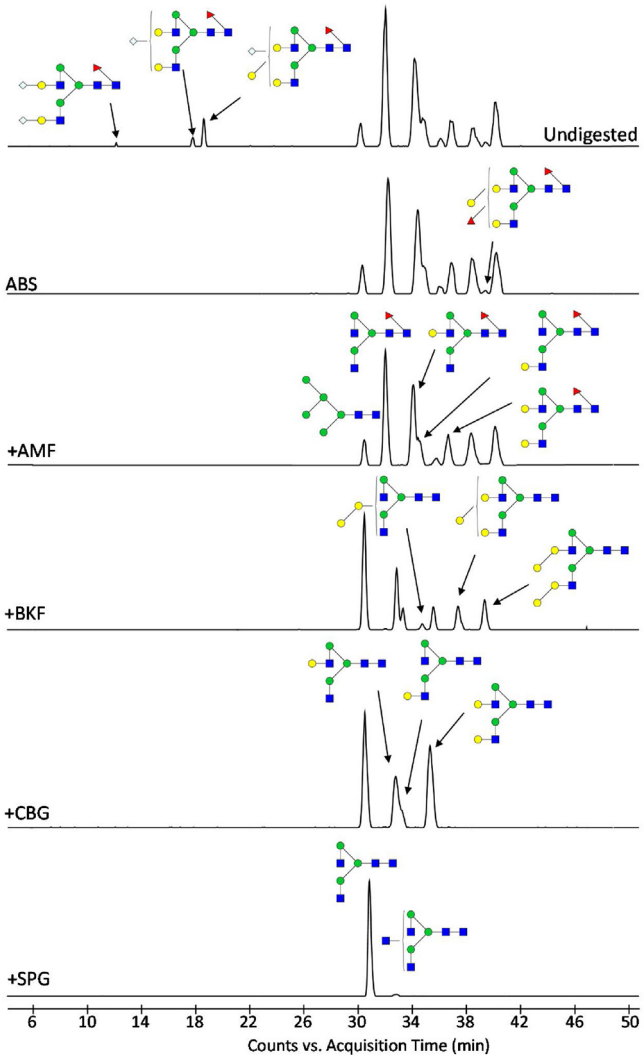



**Fig. 1.** Sequential exoglycosidase digestions of 2-AA labelled Cetuximab N-glycans analyzed by CE-MS.

**Table 2**
Identified Cetuximab N-glycan structures originating from Fd and Fc fragments.

| Structures | m/z | Fd | Fc |
|---|---|---|---|
| FA2G2S2 | 1259.82 | Yes | No |
| FA3G3GA1S2 | 1523.53 | Yes | No |
| FA2G1S1 | 1025.24 | Yes | No |
| FA2G2S1 | 1106.28 | Yes | No |
| FA2G2GA1S1 | 1187.8 | Yes | Yes |
| FA3G3GA2S1 | 1451.89 | Yes | No |
| M5 | 676.65 | Yes | Yes |
| FA1 | 689.16 | Yes | Yes |
| A2 | 717.77 | No | Yes |
| M6 | 757.75 | Yes | Yes |
| FMan4A1 | 770.2 | Yes | Yes |
| FA2 | 790.7 | Yes | Yes |
| FM5A1 | 851.3 | Yes | Yes |
| FA2(3)G1 | 871.72 | Yes | Yes |
| FA2(6)G1 | 871.72 | Yes | Yes |
| FA2G1GA1 | 952.75 | Yes | Yes |
| FMan5G1 | 932.22 | Yes | Yes |
| FA2G2 | 952.75 | Yes | Yes |
| FMan5G1GA1 | 1013.37 | Yes | Yes |
| FA2G2GA1 | 1033.76 | Yes | Yes |
| FA2FG2GA1 | 1106.89 | Yes | Yes |
| FA3G2 | 1054.27 | Yes | No |
| FA2G2GA2 | 1115.28 | Yes | Yes |
| FA3G3GA3 | 1378.89 | Yes | No |

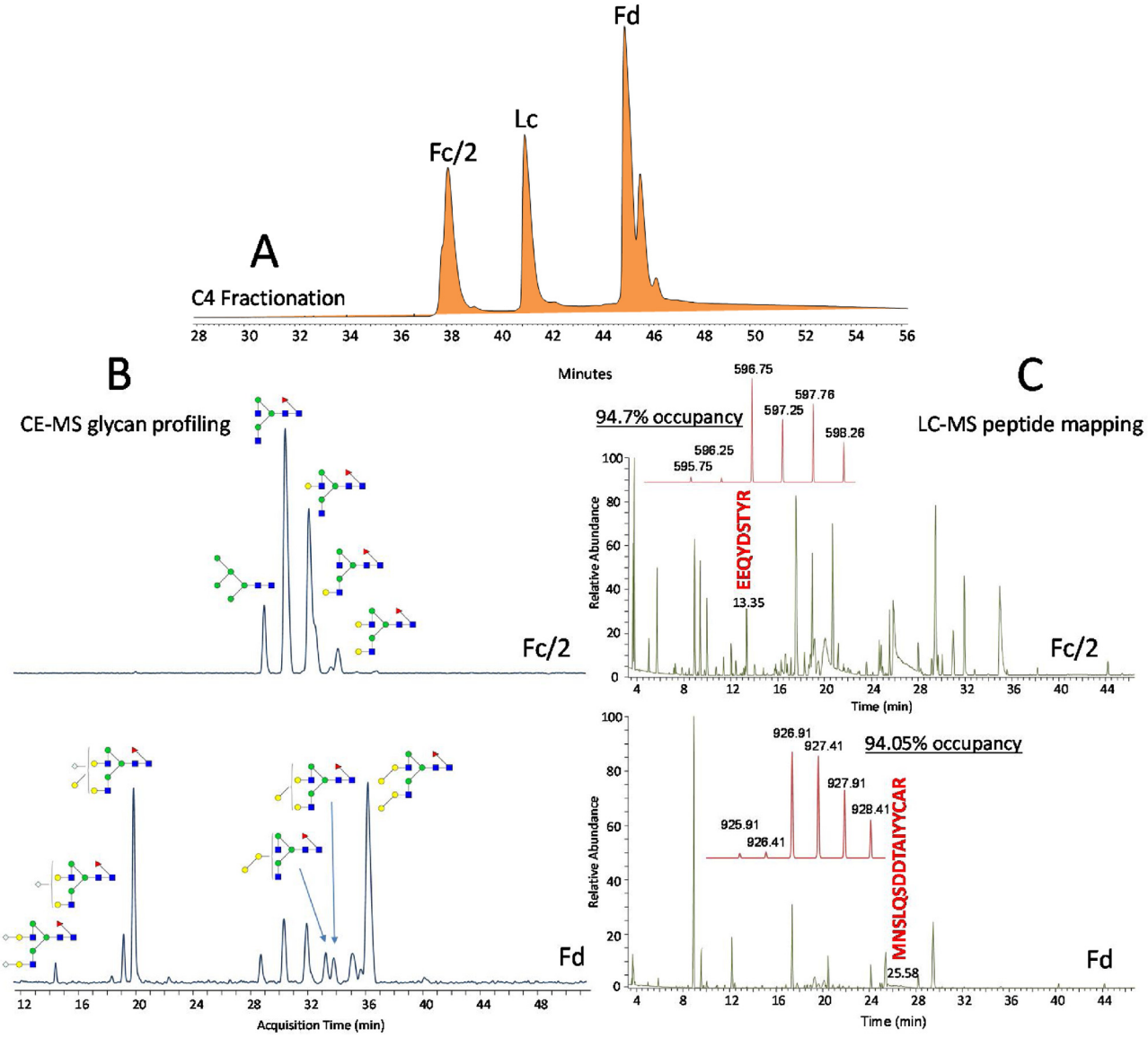



**Fig. 2.** C4 reverse phase fractionation of reduced and Fabricator digested Cetuximab followed by CE-MS glycoprofiling and LC-MS peptide mapping.

The deglycosylated fragments were further trypsin digested prior to LC–MS peptide mapping analysis allowing the identification of potential glycosylation sites due to the conversion of glycosylated asparagine residues into $^{18}O$ labeled aspartic acid residues. Peptide mapping sequence coverage was 95% on the Fd, 92.9% on the Fc/2 and 100% on the Lc fragment. In agreement with the literature, potential glycosylation sites were found at Asn 88 (Fig. 2C, MNSLQS$^{18}$DDTAIYYCAR) and Asn 299 (Fig. 2C, EEQY$^{18}$DSTYR-Fc fragment). Using the relative ratio of extracted ion chromatograms from the heavy-light (glycosylated-nonglycosylated peptides) doublets, site occupancy was calculated based on the $^{16/18}O$ levels where 94.05% site occupancy was identified on the Fd and 94.7% on the Fc/2 fragment.

### 3.3. Charge variant analysis

MAbs are the products of a long manufacturing process wherein various modifications can occur on the primary sequence due to enzymatic or chemical mechanisms. Sialylation, deamidation and C-terminal lysine cleavage can increase the net surface charge of the proteins thus decreasing their pI values resulting in the formation acidic variants. Basic variants can originate from the presence of C-terminal lysine, succinimide formation, and desialylation by the removal of negative and addition of positive charge. Compared to other mAbs Cetuximab has a reportedly complex charge variant profile due to heterogeneity arising from N-glycosylation bearing sialylation and additional modifications such as C-terminal lysine residues. To investigate the contribution of the N-glycosylation present, in addition to other primary sequence based PTMs, cation exchange chromatography was performed using pH gradient elution to separate the charge variants of Cetuximab followed by N-glycan profiling. As is shown in Fig. 3A, 8 main fractions were separated and collected using cation exchange chromatography. Glycan traces obtained from the indicated charge variants are shown in Fig. 3B suggesting the impact of sialic acid to the charge variant profile. Focusing on sialylation and α-galactosylation, an interesting trend was found between the glycosylation profiles of the different charge variants. On the acidic variants (1–4) a higher sialylation level was found, the main Cetuximab charge variant (5) showed a ~50–50% sialylation-α-galactosylation level, while this ratio was shifted towards to the α-galactosylation on the basic variants. These results suggest that glycosylation has a crucial effect on

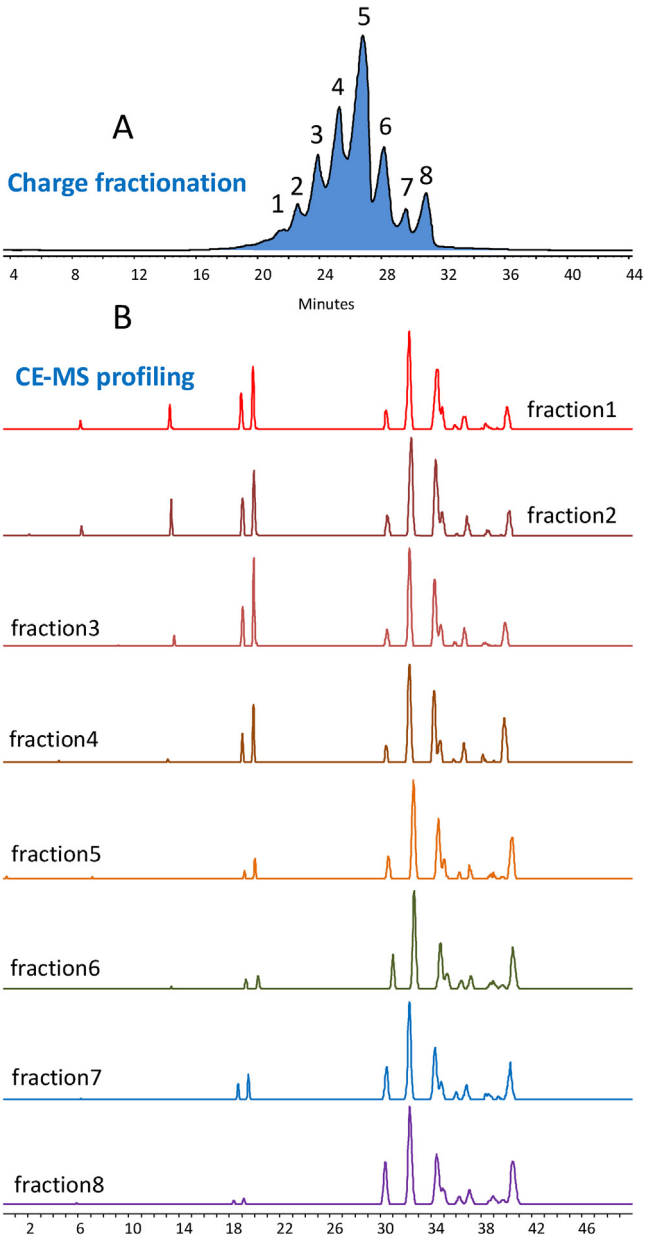



**Fig. 3.** Linear pH gradient cation-exchange chromatography based fractionation of Cetuximab charge variants followed by CE-MS glycoprofiling.

the net charge characteristics of the protein which can alter affinity to the Fc receptors.

## 4. Conclusions

Cetuximab glycosylation was examined in this study using multiple fractionation and digestion strategies with CE-MS profiling and LC-MS peptide mapping. Glycan release was performed in heavy water which enables identification of potential glycosylation sites with their relative site occupancy. N-glycans were annotated by the combination of exoglycosidase sequencing and CE-MS. Site-specific glycoprofiling suggested that glycans with terminal NGNA and α-Gal are located on the Fd fragment while the Fc/2 glycans are core-fucosylated bi-antennary structures with different level of β-galactosylation. Cetuximab glycosylation was also examined across charge based variants using cation exchange chromatography with linear pH gradient showing altered sialylation and α-galactosylation levels suggesting the impact of glycans on the surface net charge of the protein.

## CRediT authorship contribution statement

**Csaba Váradi:** Methodology, Formal analysis, Data curation, Visualization, Writing - original draft. **Craig Jakes:** Data curation, Formal analysis, Methodology, Writing - review & editing. **Jonathan Bones:** Conceptualization, Supervision, Writing - review & editing, Project administration, Funding acquisition.

## Declaration of Competing Interest

The authors declare no conflict of interest.

## Acknowledgement

The authors gratefully acknowledge funding from EU Framework Programme 7 under Marie Curie Actions, grants reference: FP7-PEOPLE-2013-ITN-608381 and the GINOP-2.3.4-15-2016-00004 project.

## References

[1] S. Demaria, E. Pikarsky, M. Karin, L.M. Coussens, Y.-C. Chen, E.M. El-Omar, G. Trinchieri, S.M. Dubinett, J.T. Mao, E. Szabo, A. Krieg, G.J. Weiner, B.A. Fox, G. Coukos, E. Wang, R.T. Abraham, M. Carbone, M.T. Lotze, Cancer and inflammation: promise for biological therapy, J. Immunother. (Hagerstown, Md. 1997) 33 (4) (2010) 335–351.
[2] B. Hintersteiner, N. Lingg, E. Janzek, O. Mutschlechner, H. Loibner, A. Jungbauer, Microheterogeneity of therapeutic monoclonal antibodies is governed by changes in the surface charge of the protein, Biotechnol. J. 11 (12) (2016) 1617–1627.
[3] G. Galizia, E. Lieto, F. De Vita, M. Orditura, P. Castellano, T. Troiani, V. Imperatore, F. Ciardiello, Cetuximab, a chimeric human mouse anti-epidermal growth factor receptor monoclonal antibody, in the treatment of human colorectal cancer, Oncogene 26 (25) (2007) 3654–3660.
[4] D.S. Goodsell, The molecular perspective: epidermal growth factor, Oncologist 8 (5) (2003) 496–497.
[5] R.N. Jorissen, F. Walker, N. Pouliot, T.P.J. Garrett, C.W. Ward, A.W. Burgess, Epidermal growth factor receptor: mechanisms of activation and signalling, Exp. Cell Res. 284 (1) (2003) 31–53.
[6] C. Xue, J. Wyckoff, F. Liang, M. Sidani, S. Violini, K.-L. Tsai, Z.-Y. Zhang, E. Sahai, J. Condeelis, J.E. Segall, Epidermal Growth Factor Receptor Overexpression Results in Increased Tumor Cell Motility In vivo Coordinately with Enhanced Intravasation and Metastasis, Cancer Res. 66 (1) (2006) 192–197.
[7] P. Seshacharyulu, M.P. Ponnusamy, D. Haridas, M. Jain, A. Ganti, S.K. Batra, Targeting the EGFR signaling pathway in cancer therapy, Expert Opin. Ther. Targets 16 (1) (2012) 15–31.
[8] D.J. Jonker, C.J. O'Callaghan, C.S. Karapetis, J.R. Zalcberg, D. Tu, H.-J. Au, S.R. Berry, M. Krahn, T. Price, R.J. Simes, N.C. Tebbutt, G. van Hazel, R. Wierzbicki, C. Langer, M.J. Moore, Cetuximab for the treatment of colorectal cancer, N. Engl. J. Med. 357 (20) (2007) 2040–2048.
[9] P. Specenier, J.B. Vermorken, Cetuximab: its unique place in head and neck cancer treatment, Biol. Targets Ther. 7 (2013) 77–90.
[10] F.S. Farhat, W. Houhou, Targeted therapies in non-small cell lung carcinoma: what have we achieved so far? Ther. Adv. Med. Oncol. 5 (4) (2013) 249–270.
[11] R. Pirker, J.R. Pereira, A. Szczesna, J. Von Pawel, M. Krzakowski, R. Ramlau, I. Vynnychenko, K. Park, C.-T. Yu, V. Ganul, Cetuximab plus chemotherapy in patients with advanced non-small-cell lung cancer (FLEX): an open-label randomised phase III trial, Lancet 373 (9674) (2009) 1525–1531.
[12] D. Reusch, M.L. Tejada, Fc glycans of therapeutic antibodies as critical quality attributes, Glycobiology 25 (12) (2015) 1325–1334.
[13] J. Qian, T. Liu, L. Yang, A. Daus, R. Crowley, Q. Zhou, Structural characterization of N-linked oligosaccharides on monoclonal antibody cetuximab by the combination of orthogonal matrix-assisted laser desorption/ionization hybrid quadrupole-quadrupole time-of-flight tandem mass spectrometry and sequential enzymatic digestion, Anal. Biochem. 364 (1) (2007) 8–18.
[14] A. Beck, H. Diemer, D. Ayoub, F. Debaene, E. Wagner-Rousset, C. Carapito, A. Van Dorsselaer, S. Sanglier-Cianférani, Analytical characterization of biosimilar antibodies and Fc-fusion proteins, Trac Trends Anal. Chem. 48 (2013) 81–95.
[15] D. Patel, X. Guo, S. Ng, M. Melchior, P. Balderes, D. Burtrum, K. Persaud, X. Luna, D.L. Ludwig, X. Kang, IgG isotype, glycosylation, and EGFR expression determine the induction of antibody-dependent cellular cytotoxicity in vitro by cetuximab, Hum. Antibodies 19 (4) (2010) 89–99.
[16] C.H. Chung, B. Mirakhur, E. Chan, Q.-T. Le, J. Berlin, M. Morse, B.A. Murphy, S.M. Satinover, J. Hosen, D. Mauro, R.J. Slebos, Q. Zhou, D. Gold, T. Hatley, D.J.

Hicklin, T.A.E. Platts-Mills, Cetuximab-induced anaphylaxis and IgE specific for Galactose-α-1,3-Galactose, N. Engl. J. Med. 358 (11) (2008) 1109–1117.
[17] F. Higel, A. Seidl, F. Sörgel, W. Friess, N-glycosylation heterogeneity and the influence on structure, function and pharmacokinetics of monoclonal antibodies and Fc fusion proteins, Eur. J. Pharm. Biopharm. 100 (2016) 94–100.
[18] P.M. Angel, J.M. Lim, L. Wells, C. Bergmann, R. Orlando, A potential pitfall in 18O-based N-linked glycosylation site mapping, Rapid Commun. Mass Spectrom. 21 (5) (2007) 674–682.
[19] C. Varadi, K. Nehez, O. Hornyak, B. Viskolcz, J. Bones, Serum n-glycosylation in Parkinson's disease: a novel approach for potential alterations, Molecules (Basel, Switzerland) 24 (12) (2019).
[20] J.W. Steinke, T.A. Platts-Mills, S.P. Commins, The alpha-gal story: lessons learned from connecting the dots, J. Allergy Clin. Immunol. 135 (3) (2015) 589–596, quiz 597.